physica status solidi rrl
www.pss-rapid.com

Excellent Passivation of *n*-Type Silicon Surfaces Enabled by Pulsed-Flow Plasma-Enhanced Chemical Vapor Deposition of Phosphorus Oxide Capped by Aluminum Oxide

Jimmy Melskens, Roel J. Theeuwes, Lachlan E. Black, Willem-Jan H. Berghuis, Bart Macco, Paula C. P. Bronsveld, and W. M. M. Kessels*

Phosphorus oxide (PO_x) capped by aluminum oxide (Al_2O_3), prepared by atomic layer deposition (ALD), has recently been introduced as a surface passivation scheme for planar *n*-type FZ silicon. In this work, a fast pulsed-flow plasma-enhanced chemical vapor deposition (PECVD) process for the PO_x layer is introduced, making it possible to increase the PO_x deposition rate significantly while maintaining the PO_x/Al_2O_3 passivation quality. An excellent surface passivation is realized on *n*-type planar FZ and Cz substrates ($J_0 = 3.0$ fA cm^{-2}). Furthermore, it is demonstrated that the PO_x/Al_2O_3 stack can passivate textured surfaces and that the application of an additional PECVD SiN_x capping layer renders the stack stable to a firing treatment that is typically used in fire-through contact formation ($J_0 = 12$ fA cm^{-2}). The excellent surface passivation is enabled by a high positive fixed charge density ($Q_f \approx 4 \times 10^{12}$ cm^{-2}) and an ultralow interface defect density ($D_{it} \approx 5 \times 10^{10}$ eV^{-1} cm^{-2}). Finally, outstanding passivation is demonstrated on textured silicon with a heavy n^+ surface doping, as is used in solar cells, on par with alnealed SiO_2. These findings indicate that PO_x/Al_2O_3 is a highly suited passivation scheme for *n*-type silicon surfaces in typical industrial solar cells.

To realize high-efficiency crystalline silicon (c-Si) solar cells it is essential to have excellent surface passivation, which is ideally achieved by combining a high degree of chemical passivation to reduce the interface defect density with field-effect passivation to strongly reduce the minority carrier concentration near the silicon surface.[1–3] While new passivating materials continue to be identified,[4] only few are known to provide good chemical passivation in combination with a high fixed charge density. A prominent example is the negative fixed charge that aluminum oxide (Al_2O_3) induces near the Si surface, which makes Al_2O_3 ideal for the passivation of *p*-type Si surfaces.[5–7] Similarly, the surface passivation and positive charge that is associated with silicon nitride (SiN_x) has made SiN_x the standard material for passivating *n*-type Si surfaces,[8] although the SiN_x films that provide the highest degree of chemical passivation typically only exhibit a mildly positive fixed charge density.[9–12]

In this context, it is interesting to consider phosphorus oxide (PO_x) capped by Al_2O_3, which was first reported as a high-quality passivation stack on indium phosphide (InP) nanowires.[13] This layer stack can also provide excellent surface passivation on c-Si, which is attributed to a low interface defect density (inferred from lifetime and high-frequency parallel conductance data) in combination with a high positive fixed charge near the c-Si surface.[14,15] In addition, there are also opportunities to achieve local contact formation by doping from the PO_x/Al_2O_3 layer stack.[16] The excellent surface passivation provided by PO_x/Al_2O_3 has so far been

Dr. J. Melskens, R. J. Theeuwes, W.-J. H. Berghuis, Dr. B. Macco, Prof. W. M. M. Kessels
Department of Applied Physics
Eindhoven University of Technology
P.O. Box 513, Eindhoven, MB 5600, The Netherlands
E-mail: j.melskens@tudelft.nl, j.melskens@tue.nl

The ORCID identification number(s) for the author(s) of this article can be found under https://doi.org/10.1002/pssr.202000399.

Dr. L. E. Black
Research School of Electrical, Energy and Materials Engineering
The Australian National University
Canberra, ACT 2600, Australia

Dr. P. C. P. Bronsveld
TNO Energy Transition
Solar Energy
Westerduinweg 3, Petten, ZG 1755, The Netherlands

DOI: 10.1002/pssr.202000399

demonstrated on lightly doped planar *n*-FZ substrates, and the influence of the PO_x film thickness as well as the annealing time and temperature on the passivation quality have been studied.[14,15] The PO_x deposition has so far been achieved using a cyclical process flow typical of atomic layer deposition (ALD). As the reactions involved in this process are not strictly self-limiting, it is labeled as an ALD-like process in the remainder of this work, following previously used terminology.[13] Potential changes to this PO_x deposition process flow to reduce the deposition time have not yet been considered. Furthermore, several aspects connected to the potential application of PO_x/Al_2O_3 in industrial solar cells remain to be investigated.

In this contribution, we discuss a fast, pulsed-flow plasma-enhanced chemical vapor deposition (PECVD) process for the PO_x layer, developed in the same ALD reactor used previously,[13–15] and we explore the passivation quality of the resulting PO_x (5 nm)/Al_2O_3 (10 nm) stacks deposited at a substrate temperature of 100 °C. This PECVD process is based on cycles, in analogy to the pulsed-flow PECVD of Al_2O_3 reported by Dingemans et al.,[17] i.e., the precursor is briefly pulsed into the oxygen plasma during each cycle. More details of the PO_x/Al_2O_3 stack fabrication are shown in **Figure 1**. As PO_x is known to be hygroscopic, it requires a capping layer to be stable in air, which in this study is a plasma ALD Al_2O_3 layer, as also used previously.[13–15] An important advantage of the PECVD process with respect to the previously used ALD-like process for the PO_x layer is the fact that it is significantly faster, i.e., the deposition time is reduced by approximately a factor of 6. There would be opportunities to reduce the deposition time even further in a fully optimized continuous PECVD process. Specifically, the total processing time is currently dominated by the O_2 plasma step: the time that the plasma is on, which has not yet been carefully optimized, is much longer than the precursor dosing step and there is a long purging step after this O_2 plasma step. In an optimized continuous PECVD process without purging steps, the total processing time could be significantly reduced. An analogous transfer from an initially slow, lab-scale, ALD process towards a fast, industrially viable PECVD process has already been realized for Al_2O_3,[7,18,19] which could similarly take place for PO_x. In addition, the precursor consumption in case of the PECVD process might be lower as

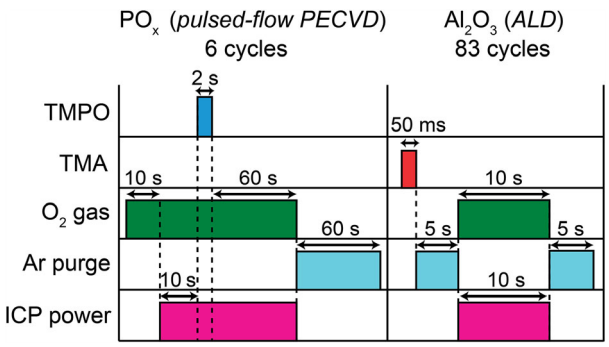

Figure 1. Schematic representation of the process used to prepare PO_x/Al_2O_3 stacks using pulsed-flow PECVD for the PO_x layer and plasma-enhanced ALD for the Al_2O_3 layer (timings not to scale). Both deposition cycles are shown, while the number of cycles is varied for each layer to arrive at the desired layer thickness.

the precursor dosing time is significantly reduced in comparison to the ALD-like process for the PO_x layer (note that the percentage of precursor consumed in both cases is not known). Regarding thickness uniformity we note that this is superior for the ALD-like process in comparison to the PECVD process (8% vs 23% thickness variation over an 8 in. round area). The relatively low uniformity is believed to be mainly due to the use of a reactor which is not optimized for uniform precursor flow (precursor injection takes place on one side of the chamber). This can, however, be circumvented when transferring this process to PECVD reactors which are designed with uniform precursor injection in mind. Furthermore, PECVD processes are attractive because they are common in industrial solar cell processing, for instance, for the fabrication of SiN_x and Al_2O_3 layers. For Al_2O_3, a high passivation quality has already been reported for layers fabricated using a pulsed-flow PECVD process developed in an ALD reactor,[17] while PECVD Al_2O_3 (combined with an integrated capping layer) is widely used as a rear side passivation technology in industrial solar cell processing.[20]

To assess the PO_x/Al_2O_3 passivation quality when using pulsed-flow PECVD as a fabrication method for the PO_x layer, we consider planar *n*-FZ as well as planar and textured *n*-Cz substrates. Furthermore, we assess the firing stability and compatibility with a SiN_x capping layer, which are critical aspects for integration of PO_x/Al_2O_3 in industrial solar cells. Finally, we consider textured *n*-Cz substrates with an *n*-type surface diffusion because the high positive fixed charge that is induced by the PO_x/Al_2O_3 stack makes it attractive for the passivation of n^+ surfaces. We thereby significantly extend the range of substrates and surfaces on which PO_x/Al_2O_3 passivation has been demonstrated compared with previous studies which only examined the passivation quality on planar FZ substrates.[14,15] To investigate the PO_x/Al_2O_3 passivation quality, we combine quasi-steady-state photoconductance (QSSPC) measurements with capacitance–voltage (*C*–*V*) analysis and corona charging experiments.

First, the passivation quality of the PO_x/Al_2O_3 stacks grown on planar *n*-type FZ substrates has been assessed using the PECVD process for the PO_x layer and compared with the previously reported ALD-like process. As shown in **Figure 2**a, both these processes yield an excellent passivation quality, with an extremely low recombination parameter of $J_0 = 3.0$ fA cm^{-2} per side for the PECVD process after postdeposition annealing in N_2 (400 °C for 10 min). This confirms that the strongly reduced deposition time for the PECVD PO_x layer does not come at the expense of a deterioration in passivation quality for the PO_x/Al_2O_3 stack with respect to the previously used ALD-like process for the PO_x layer. Note that the annealing treatment is needed to activate the surface passivation because there is no significant surface passivation in the as-deposited state (e.g., $\tau_{eff} < 10$ µs in case of PECVD PO_x/ALD Al_2O_3).

Second, the passivation quality of PO_x/Al_2O_3 capped by SiN_x (75 nm) has been evaluated on planar and textured Cz substrates after a postdeposition firing treatment that is typical for fire-through contact metallization. Note here that textured substrates are generally more challenging to passivate than planar substrates, while textured Cz substrates with a SiN_x capping layer as antireflection coating are standardly used in industrial solar cells. As shown in Figure 2b, when applying a SiN_x capping layer and firing the resulting $PO_x/Al_2O_3/SiN_x$ layer stack, an excellent

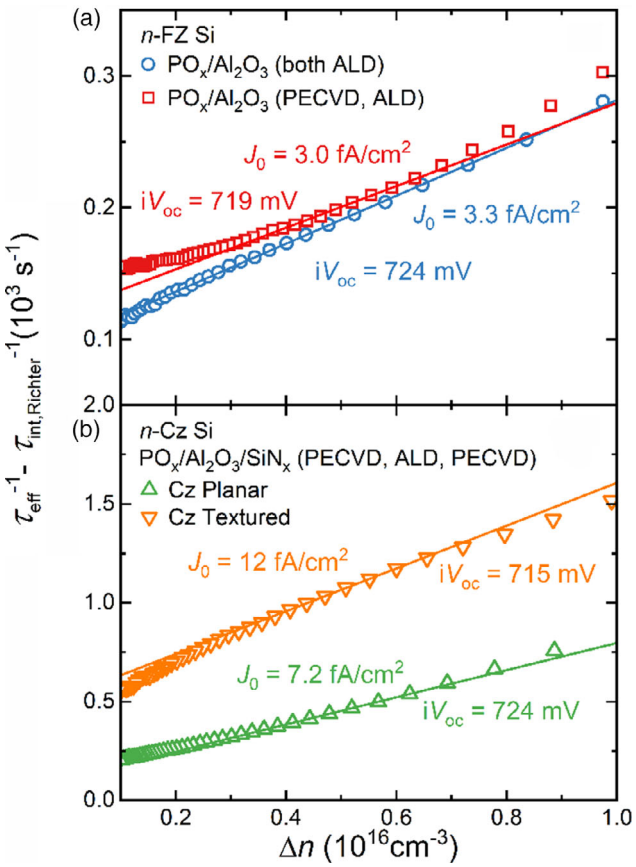

Figure 2. Inverse Auger-corrected (parametrization by Richter et al.[40]) lifetime curves for symmetric PO$_x$/Al$_2$O$_3$ lifetime samples. a) PO$_x$ was deposited using the ALD-like process (data adapted from Black and Kessels[15]) or the PECVD process on planar *n*-FZ substrates and the PO$_x$/Al$_2$O$_3$ stacks were subsequently annealed in N$_2$. b) PECVD SiN$_x$ was symmetrically deposited on the PO$_x$/Al$_2$O$_3$ stacks on planar and textured *n*-Cz substrates and a firing treatment typical for fire-through contact formation was subsequently used. The J_0 values shown next to the curves have been fitted at $\Delta n = 5 \times 10^{15}$ cm^{-3} and correspond to one side of the samples.

passivation can be reached on both planar ($J_0 = 7.2$ fA cm^{-2}) and textured ($J_0 = 12$ fA cm^{-2}) Cz substrates. We also report the corresponding implied open-circuit voltage (iV_{oc}) values here, as this parameter includes the wafer bulk quality and any light in-coupling effects that play a role in solar cells in addition to the surface passivation quality. The high passivation quality after SiN$_x$ capping and subsequent firing is thought to be due to the SiN$_x$ layer that can act both as a hydrogenation source and a hydrogen effusion barrier. This hypothesis is supported by the fact that the passivation quality of PO$_x$/Al$_2$O$_3$ stacks without SiN$_x$ capping layer does not improve but rather degrades after firing (J_0 can increase by ≈20 fA cm^{-2}). Such loss of passivation upon annealing or firing is often attributed to effusion of hydrogen from the film and interface and comparable cases have been reported for Al$_2$O$_3$[7] as well as poly-Si[21] and ZnO[22] with and without capping layer. In addition, when depositing the SiN$_x$ layer, an increase in J_0 of ≈20–40 fA cm^{-2} can be observed, which can be largely repaired by the firing treatment, thus explaining the difference in J_0 for the planar samples

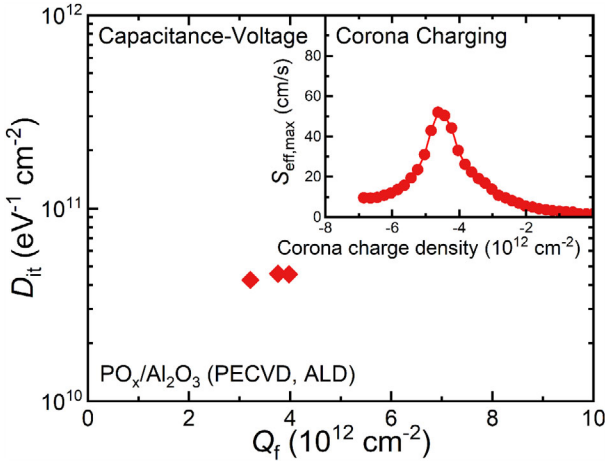

Figure 3. Interface defect density (D_{it}) and fixed charge density (Q_f) as determined using quasi-static capacitance–voltage (*C*–*V*) characterization using three separate measurements conducted on the same PO$_x$/Al$_2$O$_3$ stack, where the PO$_x$ layer was deposited using the PECVD process on a planar *n*-FZ substrate and annealed in N$_2$. The inset shows a corona-lifetime characterization of the same layer stack fabricated symmetrically on a planar *n*-FZ substrate, also after annealing in N$_2$.

without and with SiN$_x$ capping layer and firing treatment, as shown in Figure 2a,b, respectively. Interestingly, in case of the textured substrates, we observe a 22 mV improvement in iV_{oc} for the fired, symmetric PO$_x$/Al$_2$O$_3$/SiN$_x$ stack compared with a fired, symmetric and optimized, industry-ready SiN$_x$ reference that was processed in the same batch.

To understand why the passivation quality of annealed stacks consisting of PECVD PO$_x$ and Al$_2$O$_3$ can reach such high levels, quasi-static *C*–*V* characterization and a combination of corona charging and lifetime measurements, i.e., corona-lifetime experiments, are used to assess both the chemical passivation in terms of the interface defect density (D_{it}) and the field-effect passivation in terms of the fixed charge density (Q_f). Note that the quasi-static measurement mode in the *C*–*V* analysis enables a more accurate determination of the D_{it} value in comparison to the previously used high-frequency mode.[14] The results of the combined *C*–*V* and corona charging analysis are shown in **Figure 3**. Multiple *C*–*V* measurements on the same PO$_x$/Al$_2$O$_3$ sample have been conducted for statistical accuracy, which provides extra support for the conclusion that the excellent passivation quality enabled by the stack is due to an exceptionally low D_{it} ($4.5 \pm 0.2 \times 10^{10}$ eV^{-1} cm^{-2}) combined with a high positive Q_f ($3.7 \pm 0.3 \times 10^{12}$ cm^{-2}). When comparing these results with D_{it} and Q_f values from the literature for a broad selection of different types of passivating Al$_2$O$_3$[23,24] ($D_{it} \approx (4-70) \times 10^{10}$ eV^{-1} cm^{-2}; $Q_f \approx -(1-10) \times 10^{12}$ cm^{-2}) and SiN$_x$[9–12] ($D_{it} \approx (6-500) \times 10^{10}$ eV^{-1} cm^{-2}; $Q_f \approx +(0.2-10) \times 10^{12}$ cm^{-2}), it is clear that PO$_x$/Al$_2$O$_3$ indeed enables a state-of-the-art passivation quality that appears highly suitable for *n*-type Si surfaces. Further confirmation of the existence of a high positive fixed charge that is induced by the annealed PO$_x$/Al$_2$O$_3$ stack is provided by the corona charging experiments which indicate that $Q_f = 4.5 \pm 0.2 \times 10^{12}$ cm^{-2}, which approximately corresponds to the Q_f value determined via *C*–*V* measurements. Here, it is noted that single-sided

samples were used for the C–V characterization, while symmetrical samples were used for the corona charging experiments, which can introduce small sample-to-sample variations in the Q_f comparison. The combination of a very low D_{it} and a high positive Q_f is particularly striking. SiN_x, which is typically used to passivate n-type Si surfaces, can also yield a low D_{it}, although this is accompanied by a rather low positive Q_f ($\approx 1 \times 10^{12}$ cm^{-2}). On the contrary, higher positive Q_f values are only attainable for SiN_x at the expense of a strongly increased D_{it}.[9–12,25,26] Electrostatic charges can yield an improved passivation quality up to charge densities of $\approx 5 \times 10^{12}$ cm^{-2} beyond which the passivation quality saturates,[27] indicating that PO_x/Al_2O_3 exhibits a nearly ideal Q_f. The undesirable trade-off between low D_{it} and high Q_f that exists for SiN_x appears to be more lenient for PO_x/Al_2O_3, which adds to the promise of the latter as a passivation scheme for n-type Si surfaces. The reason why a combination of low D_{it} and high Q_f can be achieved with PO_x/Al_2O_3 is not fully understood yet. It is, however, likely that a hydrogenation of the Si surface by the stack is responsible for the low D_{it}. More specifically, for the PO_x/Al_2O_3 stack it is plausible that there is a significant presence of —OH groups and that the hydrogen that is bonded in this way can contribute to the surface passivation. This would be similar to Al_2O_3 for which it is well established that some of the hydrogen in —CH_3 groups in the trimethylaluminum (TMA) precursor ends up as —OH groups in the film and this H can provide interface passivation.[7] This hydrogenation can be especially effective when the PO_x/Al_2O_3 stack is capped by a hydrogen-rich layer like SiN_x. The latter can act not only as a hydrogenation source, but also as a hydrogen effusion barrier for the underlying PO_x/Al_2O_3 stack. On a microscopic level, the high Q_f could be related to the presence of the diamagnetic $[(O^-)_4P]^+$ defect center in PO_x as a possible origin for the positive fixed charge density, as suggested previously.[14]

To investigate the potential of PO_x/Al_2O_3 as a passivation scheme further, we finally explore its passivation quality on n-type Si substrates with an n^+ diffused surface. These kinds of surfaces benefit from a high positive Q_f (together with a low D_{it}) and they occur in practical solar cells, e.g., the n^+ layer on the front side of a passivated emitter rear contact (PERC) solar cell. Given this context, we investigate the passivation quality on textured n-type Cz substrates with two different n-type surface diffusions: a relatively light surface diffusion ($R_{sheet} = 260 \pm 7\,\Omega\square^{-1}$) and a heavier surface diffusion ($R_{sheet} = 137 \pm 7\,\Omega\square^{-1}$). The symmetric PO_x/Al_2O_3 samples on n^+ Si are annealed in N_2 at 400 °C to assess the passivation quality. The results for both the 137 and 260 $\Omega\square^{-1}$ substrates are shown in **Figure 4**a and clearly indicate excellent J_0 values for passivated diffused n^+ surfaces, with values of 30 and 12 fA cm^{-2} per side, respectively, after annealing.

To put these results into perspective, it is worthwhile to compare the PO_x/Al_2O_3 passivation on n^+ Si with a variety of state-of-the-art passivation schemes based on SiN_x or SiO_2 reported in the literature[28–32] which were also fabricated on textured n-Cz substrates with different levels of n^+ surface doping resulting in different R_{sheet} values. This comparison is shown in Figure 4b and illustrates that the passivation quality of PO_x/Al_2O_3 surpasses the passivation quality of SiN_x on textured n^+ Si surfaces and is on par with state-of-the-art alnealed SiO_2 as

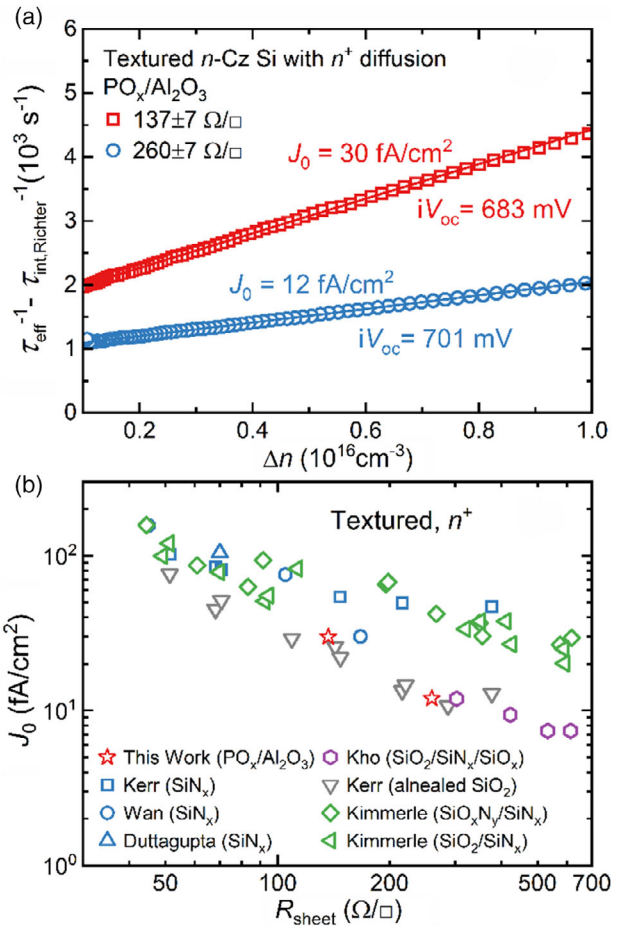

Figure 4. a) Inverse Auger-corrected (parametrization by Richter et al.[40]) lifetime curves for symmetric PO_x/Al_2O_3 lifetime samples. The PO_x layer has been deposited on textured n-Cz substrates with two different n^+ diffusions after annealing in N_2. The J_0 values shown next to the curves have been fitted at $\Delta n = 5 \times 10^{15}$ cm^{-3} and correspond to one side of the samples. b) Comparison of J_0 values for PO_x/Al_2O_3 and a variety of state-of-the-art passivation schemes from the literature[28–32] on textured n-Cz substrates with different levels of n^+ surface doping resulting in different R_{sheet} values.

well as ONO ($SiO_2/SiN_x/SiO_2$) stacks. This latter result is especially excellent and illustrates the promise of PO_x/Al_2O_3 as a candidate passivation scheme for n^+ Si surfaces. These combined findings underline that PO_x/Al_2O_3 is not only promising in the context of planar, lowly doped n-type regions, but also for the passivation of textured n^+ diffused Si surfaces. Hereby we remark that the passivation quality of a $PO_x/Al_2O_3/SiN_x$ stack on textured n^+ diffused Si surfaces as well as the compatibility with metallization schemes still need to be evaluated before the promise of PO_x/Al_2O_3 as demonstrated in this work can prove to bring a benefit as a passivation scheme to, for instance, p-type PERC solar cells.

In conclusion, a fast, pulsed-flow PECVD process has been introduced to deposit PO_x, and it is shown that a high passivation quality on various n-type Si substrates can be achieved when capping this PO_x layer by Al_2O_3. More specifically, excellent surface passivation is demonstrated on planar FZ substrates

($J_0 = 3.0\,\mathrm{fA\,cm^{-2}}$). High-quality surface passivation on planar and textured Cz substrates is also demonstrated for PO_x/Al_2O_3 stacks capped with PECVD SiN_x after a firing treatment that is typical for screen-printed metallization of silicon solar cells. The excellent level of surface passivation is enabled by a combination of chemical and field-effect passivation, as illustrated by *C–V* analysis and corona charging experiments ($D_{it} \approx 5 \times 10^{10}\,\mathrm{eV^{-1}\,cm^{-2}}$ and $Q_f \approx 4 \times 10^{12}\,\mathrm{cm^{-2}}$). Finally, an excellent surface passivation quality is demonstrated on n^+ textured Si surfaces, on par with state-of-the-art alnealed SiO_2 and ONO stacks. Together these findings underline the promise of PO_x/Al_2O_3 as a passivation scheme for *n*-type Si surfaces, with a particular appeal for the passivation of n^+ diffused regions in industrial solar cells.

Experimental Section

Sample Preparation: PO_x films with a 5 nm target thickness were deposited at a substrate temperature of 100 °C in an Oxford Instruments FlexAL ALD reactor equipped with a remote inductively coupled plasma source using trimethyl phosphate (TMPO; $PO(OCH_3)_3$) as the phosphorus precursor and an O_2 plasma as the oxygen source. PO_x was deposited in a cyclical fashion using a pulsed-flow PECVD process in which a TMPO pulse was injected during the O_2 plasma step (six cycles). Details of the PECVD process are shown in Figure 1. ALD Al_2O_3 was deposited as a capping layer with a 10 nm target thickness (83 cycles) immediately following the PO_x deposition in the same reactor at the same substrate temperature using TMA ($Al(CH_3)_3$) as the Al precursor and an O_2 plasma as the oxygen source. Symmetric lifetime test structures with PO_x/Al_2O_3 stacks were prepared on 280 µm-thick double-side polished 1–5 Ω cm 4 in. *n*-type FZ Si (100) wafers as well as 140–185 µm-thick textured and planar (double-side polished with or without random pyramid texturization through alkaline etching) 2.6–4.2 Ω cm 6 in.^{2} *n*-type Cz Si (100) wafers. Furthermore, 145 µm-thick textured symmetric n^+ Si substrates were fabricated on 1.3 Ω cm 6 in.^{2} *n*-type Cz Si (100) wafers using a phosphorus diffusion in a tube furnace, yielding sheet resistance values of 137 ± 7 and $260 \pm 7\,\Omega\,\square^{-1}$ as measured by a four-point probe setup. These substrates underwent a treatment in hydrofluoric acid (HF; 5%, 5 min) prior to the PO_x/Al_2O_3 deposition to remove the phosphosilicate glass that is formed as a consequence of the phosphorous diffusion. All substrates received a standard Radio Corporation of America (RCA) clean[33] and were etched in diluted HF (1%, 1 min) just before being loaded in the ALD reactor. Immediately prior to the PO_x deposition, an O_2 plasma (1 min, 15 mTorr, 200 W) was used in the ALD reactor to form a well-defined thin (≈1 nm) interfacial SiO_x layer between the PO_x layer and the substrate for all samples investigated in this work. This means that all PO_x/Al_2O_3 stacks are in fact $SiO_x/PO_x/Al_2O_3$ stacks, although they are labeled as PO_x/Al_2O_3 for brevity. Postdeposition annealing was performed for 10 min in N_2 at 400 °C using a Jipelec rapid thermal processing system. Some PO_x/Al_2O_3 samples on Cz substrates were symmetrically capped by 75 nm PECVD SiN_x with a refractive index of 2.03 ± 0.03 at 633 nm deposited at 375 °C using a Meyer Burger MAiA PECVD system. To assess the firing stability of these $PO_x/Al_2O_3/SiN_x$ stacks, a subsequent firing treatment was conducted using a belt furnace that is typically used for contact formation using fire-through metallization paste (1 min firing profile, 720 °C peak temperature).

Characterization: The layer thicknesses were monitored in situ by spectroscopic ellipsometry using a J. A. Woollam M-2000F UV–Vis ellipsometer (1.25–5 eV) with Sellmeier and Cauchy models for the PO_x and Al_2O_3 layers, respectively. A Sinton WCT-120TS QSSPC setup was used to assess the passivation quality and J_0 values were derived using the Kane–Swanson approach.[34] A Corona Charging System of Delft Spectral Technologies was used to conduct corona-lifetime experiments using a voltage of −10 kV applied to a tungsten needle in the setup to deposit negative charges on both sides of the PO_x/Al_2O_3 samples during subsequent 10 s charging treatments that were alternated with QSSPC measurements. The amount of deposited charge was measured after each charging step by a Kelvin probe that is part of the Corona Charging System. Q_f was derived from the deposited charge corresponding to the maximum in effective surface recombination velocity, which is typically reached when the fixed charge introduced by the passivation layer(s) is matched by the amount of deposited corona charges with the opposite sign. This method has also been applied to determine Q_f for Al_2O_3[7,35] and SiN_x[7,36] while assuming a linear charge rate that is obtained from the Kelvin probe voltage as a function of charging time before the surface goes into inversion.[37] For the *C–V* characterization, the PO_x/Al_2O_3 layer stack was fabricated on one side of the substrate and Al contacts with a 700 µm diameter were thermally evaporated through a shadow mask on the annealed PO_x/Al_2O_3 stacks. GaIn eutectic paste was applied to form an ohmic rear contact to the side of the wafer without PO_x/Al_2O_3. High-frequency (1 MHz) and quasi-static *C–V* measurements were performed using an HP 4284A precision LCR meter and HP 4140B picoammeter/DC voltage source. D_{it} was derived from the quasi-static capacitance following Berglund[38] and Q_f was inferred from the flatband voltage shift, as has been described elsewhere in more detail.[39]

Acknowledgements

The authors would like to gratefully acknowledge Dr. R. Niemann and Dr. F. Fertig from Hanwha Q-Cells GmbH for providing the *n*-type diffused substrates and E. Hoek and M. K. Stodolny from TNO Energy Transition for technical support with the SiN_x depositions and the subsequent firing stability investigation. The authors are grateful for the financial support from the Dutch Ministry of Economic Affairs via the Top-consortia Knowledge and Innovation (TKI) Program "Transparent Passivating Contact Design for Advanced Solar Cells" (RADAR; TEUE116905) and "Material Independent Rear Passivating Contact Solar Cells" (MIRACLE; TEUE116139). The work of J.M. and B.M. was supported by the Netherlands Organisation for Scientific Research under the Dutch TTW-VENI Grants 15896 and 16775, respectively. The work of L.E.B. was supported by the Australian Renewable Energy Agency (ARENA) through project RND017.

Conflict of Interest

The authors declare no conflict of interest.

Keywords

aluminum oxide, chemical vapor deposition, phosphorus oxide, silicon, surface passivation

Received: August 20, 2020
Revised: October 5, 2020
Published online: November 6, 2020

[1] U. Würfel, A. Cuevas, P. Würfel, *IEEE J. Photovoltaics* **2015**, *5*, 461.
[2] J. Melskens, B. W. H. van de Loo, B. Macco, L. E. Black, S. Smit, W. M. M. Kessels, *IEEE J. Photovoltaics* **2018**, *8*, 373.
[3] A. Cuevas, Y. Wan, D. Yan, C. Samundsett, T. Allen, X. Zhang, J. Cui, J. Bullock, *Sol. Energy Mater. Sol. Cells* **2018**, *184*, 38.
[4] L. E. Black, B. W. H. van de Loo, B. Macco, J. Melskens, W. J. H. Berghuis, W. M. M. Kessels, *Sol. Energy Mater. Sol. Cells* **2018**, *188*, 182.
[5] B. Hoex, S. B. S. Heil, E. Langereis, M. C. M. van de Sanden, W. M. M. Kessels, *Appl. Phys. Lett.* **2006**, *89*, 042112.

[6] G. Agostinelli, A. Delabie, P. Vitanov, Z. Alexieva, H. F. W. Dekkers, S. de Wolf, G. Beaucarne, *Sol. Energy Mater. Sol. Cells* **2006**, *90*, 3438.
[7] G. Dingemans, W. M. M. Kessels, *J. Vac. Sci. Technol. A* **2012**, *30*, 040802.
[8] C. Leguijt, J. A. Eikelboom, A. W. Weeber, F. M. Schuurmans, W. C. Sinke, P. F. A. Alkemade, P. M. Sarro, C. H. M. Mar, L. A. Verhoef, *Sol. Energy Mater. Sol. Cells* **1996**, *40*, 297.
[9] F. M. Schuurmans, A. Schönecker, J. A. Eikelboom, W. C. Sinke, in *Proc. of the 25th IEEE Photovoltaic Specialists Conf.*, IEEE, Piscataway, NJ, USA **1996**, pp. 485–488.
[10] S. Garcia, I. Martil, G. Gonzalez Diaz, E. Castan, S. Dueñas, M. Fernandez, *J. Appl. Phys.* **1998**, *83*, 332.
[11] M. W. P. E. Lamers, K. T. Butler, J. H. Harding, A. W. Weeber, *Sol. Energy Mater. Sol. Cells* **2012**, *106*, 17.
[12] Y. Wan, K. R. McIntosh, A. F. Thomson, *AIP Adv.* **2013**, *3*, 032113.
[13] L. E. Black, A. Cavalli, M. A. Verheijen, J. E. M. Haverkort, E. P. A. M. Bakkers, W. M. M. Kessels, *Nano Lett.* **2017**, *17*, 6287.
[14] L. E. Black, W. M. M. Kessels, *Appl. Phys. Lett.* **2018**, *112*, 201603.
[15] L. E. Black, W. M. M. Kessels, *Sol. Energy Mater. Sol. Cells* **2018**, *185*, 385.
[16] L. E. Black, M. Ernst, R. J. Theeuwes, J. Melskens, D. Macdonald, W. M. M. Kessels, *Sol. Energy Mater. Sol. Cells* **2020**, *217*, 110717.
[17] G. Dingemans, M. C. M. van de Sanden, W. M. M. Kessels, *Plasma Process. Polym.* **2012**, *9*, 761.
[18] P. Saint-Cast, J. Benick, D. Kania, L. Weiss, M. Hofmann, J. Rentsch, R. Preu, S. W. Glunz, *IEEE Electron Device Lett.* **2010**, *31*, 695.
[19] *High Efficiency Cell Technologies – From PERC to Passivated Contacts and HJT*, TaiyangNews **2019**.
[20] *International Technology Roadmap for Photovoltaics (ITRPV)*, 11th ed., **2020**; available from https://itrpv.vdma.org/viewer/-/v2article/render/48393879.
[21] B. W. H. van de Loo, B. Macco, M. Schnabel, M. K. Stodolny, A. A. Mewe, D. L. Young, W. Nemeth, P. Stradins, W. M. M. Kessels, *Sol. Energy Mater. Sol. Cells* **2020**, *215*, 110592.
[22] B. W. H. van de Loo, B. Macco, J. Melskens, W. Beyer, W. M. M. Kessels, *J. Appl. Phys.* **2019**, *125*, 105305.
[23] G. Dingemans, N. M. Terlinden, D. Pierreux, H. B. Profijt, M. C. M. van de Sanden, W. M. M. Kessels, *Electrochem. Solid-State Lett.* **2011**, *14*, H1.
[24] L. E. Black, K. R. McIntosh, *Appl. Phys. Lett.* **2012**, *20*, 202107.
[25] D. E. Aspnes, *Am. J. Phys.* **1982**, *50*, 704.
[26] W. L. Warren, P. M. Lenahan, J. Kanicki, *J. Appl. Phys.* **1991**, *70*, 2220.
[27] K. J. Weber, H. Jin, C. Zhang, N. Nursam, W. E. Jellett, K. R. McIntosh, in *Proc. of the 24th European Photovoltaic Solar Energy Conf.*, WIP, Munich, Germany **2009**, pp. 534–537.
[28] M. J. Kerr, J. Schmidt, A. Cuevas, J. Bultman, *J. Appl. Phys.* **2001**, *89*, 3821.
[29] S. Duttagupta, F. Ma, B. Hoex, T. Mueller, A. G. Aberle, *Energy Procedia* **2012**, *15*, 78.
[30] Y. Wan, D. Yan, A. Cuevas, K. R. McIntosh, in *Proc. of the 40th IEEE Photovoltaic Specialists Conf.*, IEEE, Piscataway, NJ, USA **2014**, pp. 3317–3321.
[31] A. Kimmerle, M. M. Rahman, S. Werner, S. Mack, A. Wolf, A. Richter, H. Haug, *J. Appl. Phys.* **2016**, *119*, 025706.
[32] T. C. Kho, K. C. Fong, M. Stocks, K. McIntosh, E. Franklin, S. P. Phang, W. Liang, A. Blakers, *Prog. Photovolt. Res. Appl.* **2020**, *28*, 1034.
[33] W. Kern, *RCA Rev.* **1970**, *31*, 187.
[34] D. E. Kane, R. M. Swanson, in *Proc. of the 18th IEEE Photovoltaic Specialists Conf.*, IEEE, Piscataway, NJ, USA **1985**, pp. 578–583.
[35] F. Werner, B. Veith, D. Zielke, L. Kühnemund, C. Tegenkamp, M. Seibt, R. Brendel, J. Schmidt, *J. Appl. Phys.* **2011**, *109*, 113701.
[36] S. Dauwe, J. Schmidt, A. Metz, R. Hezel, in *Proc. of the 29th IEEE Photovoltaic Specialists Conf.*, IEEE, Piscataway, NJ, USA **2002**, pp. 162–165.
[37] K. R. McIntosh, L. E. Black, S. C. Baker-Finch, T. C. Kho, Y. Y. Wan, *Energy Procedia* **2012**, *15*, 162.
[38] C. N. Berglund, *IEEE Trans. Electron Devices* **1966**, *13*, 701.
[39] L. E. Black, *Ph.D. Dissertation*, The Australian National University, Canberra, Australia **2015**.
[40] A. Richter, S. W. Glunz, F. Werner, J. Schmidt, A. Cuevas, *Phys. Rev. B* **2012**, *86*, 165202.